CT and MRI of aggressive lymphoma

G. Gavelli

U.O. RADIOLOGIA
D. Barone
G. Bandi
D. Oboldi
F. Ferroni
A. Rossi
E. Amadori
D. Diano

MEDICAL PHISICIST
F. Marcocci

Conflicts of interest: none

Contrast enhanced computed tomography (CT) has long been the imaging technique most commonly used for staging and follow up of malignant lymphoma ….

CT does not provide functional or metabolic information.

CT SCAN: the role of CT scan in L is multi fold

It is used to:

- define the full extent of disease to permit accurate staging;
- assist in treatment planning (determin the site of nodal biopsy, create radiation planning portals, select chemotherapy protocols):
- evaluate response to therapy;
- monitor patient.

CT SCAN – limited accuracy

- Small LN may harbor malignant cells;
- Larger LN may be benign;
- Significance of > number of normal size LN, in the initial early staging CT; ???
- The growth becames evident if serial studies are completed;
- Small difference in measures (≅ 15%) in near normal size LN is often related to “plane of section” artifact;
- Limited accuracy for assessing L in bone marrow;
- Inability to differentiate active disease within a residual mass;
- Limited ability to assess early response to treatment.

Spectrum of imaging features

MEDIASTINAL (HL 85%; NHL 45%)

Presence of a discrete anterior mediastinal mass with a lobulated contour …

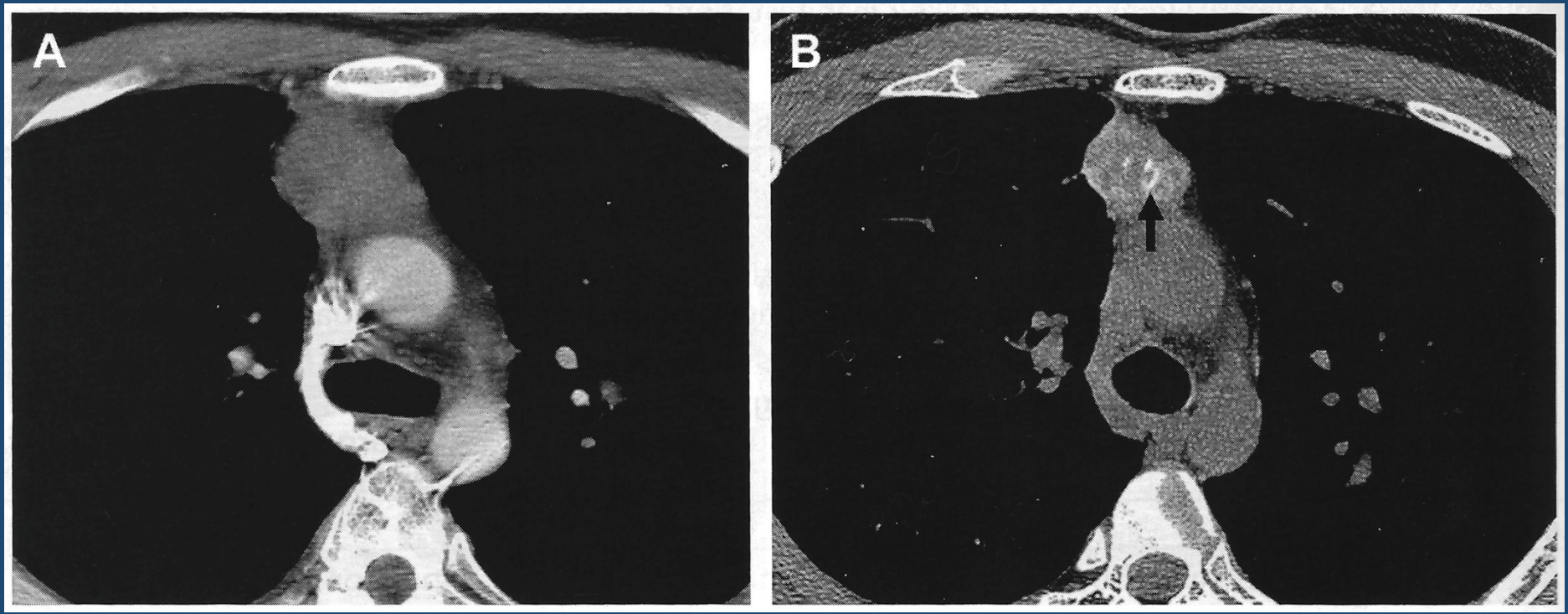

Non-Hodgkin lymphoma (diffuse large B-cell type) in a 29-year-old man.

A) Transverse mediastinal window CT (7.0-mm section thickness) scan obtained at level of azygos arch shows homogeneous soft tissue mass in anterior mediastinum.

B) CT scan obtained at the same level as A 13 months after completion of radiation therapy demonstrates that tumor has decreased in size and contains dystrophic calcifications (arrow) within remaining tumor.

23 year old woman with primary mediastinal large B-cell lymphoma (PMBCL)

Before therapy

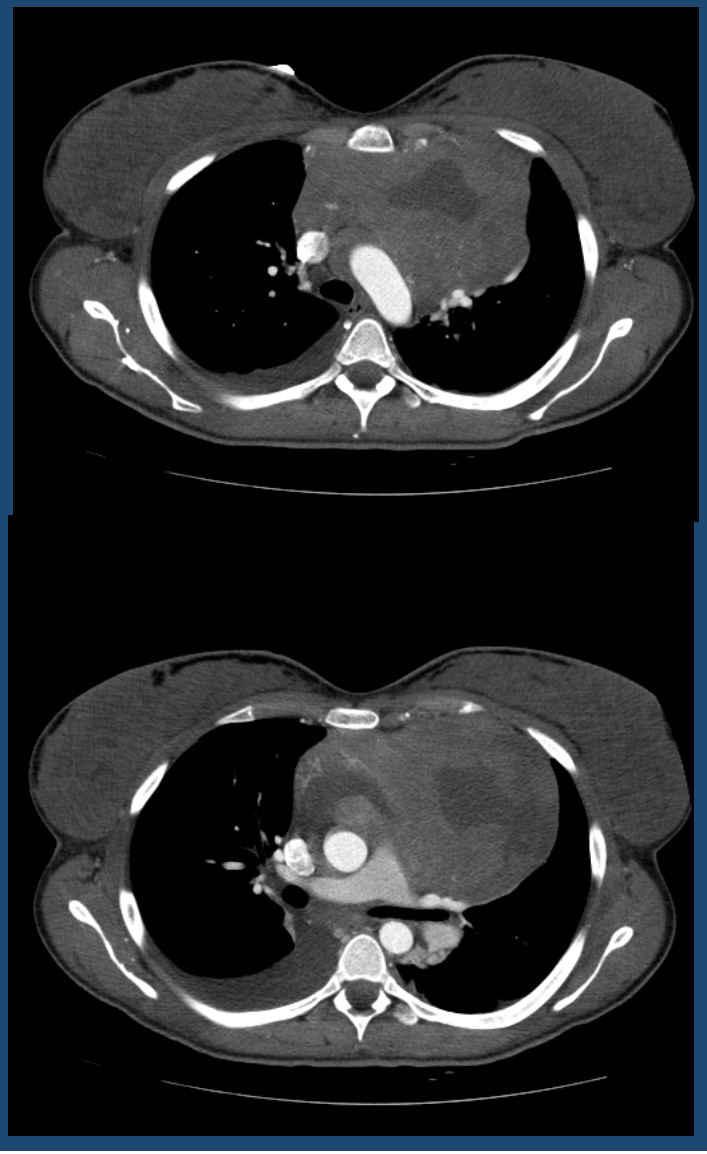

After chemotherapy and RT

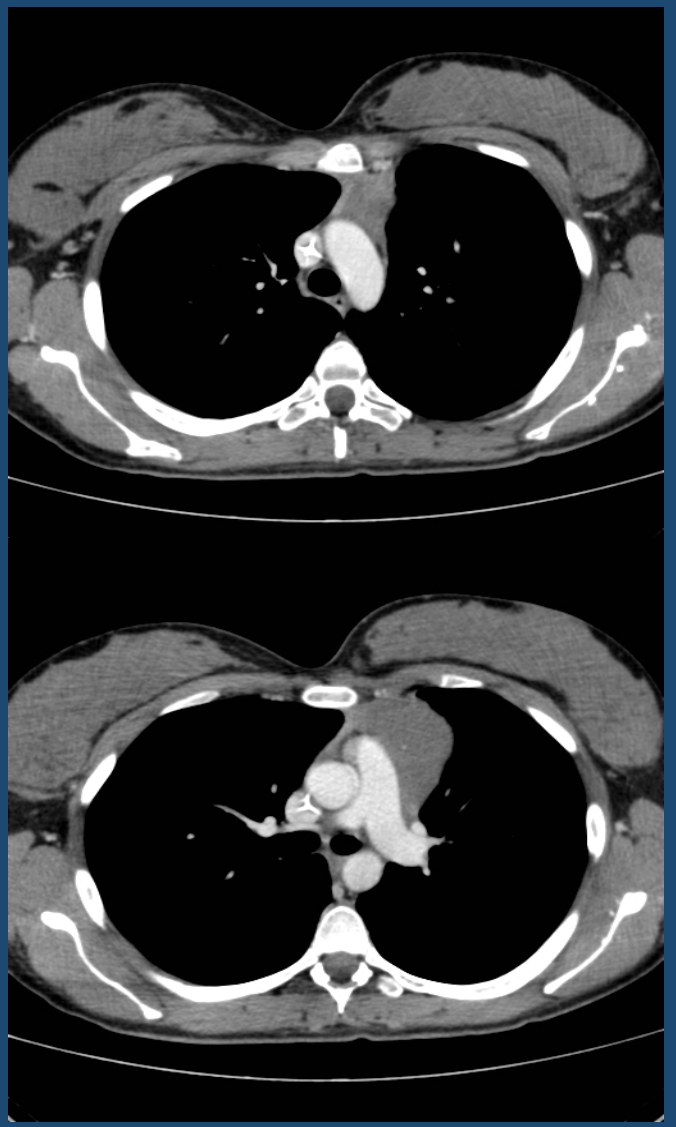

- It is difficult to differentiate HL from NHL on the basis of a nodal distribution alone;
- The sole mediastinum involvement occurs in only 5% of L cases
- Large tumors commonly contain areas of low attenuation due to hemorrhage or necrosis;
- Large B-cell L and Lymphoblastic L are the most common subtypes, primarily involving the anterior mediastinum;

30 year old man with primary mediastinal large B-cell lymphoma (PMBCL) stage IIb

Before thrapey

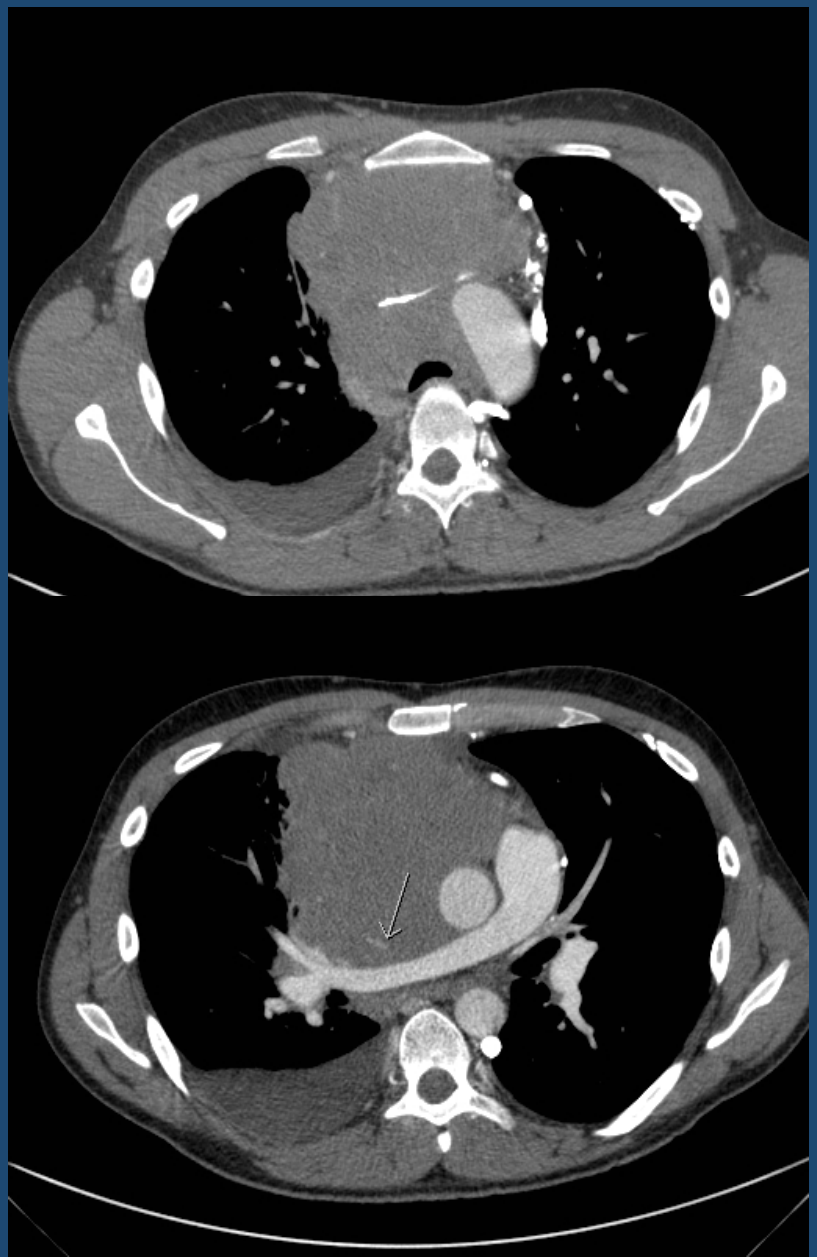

After chemotherapy and RT

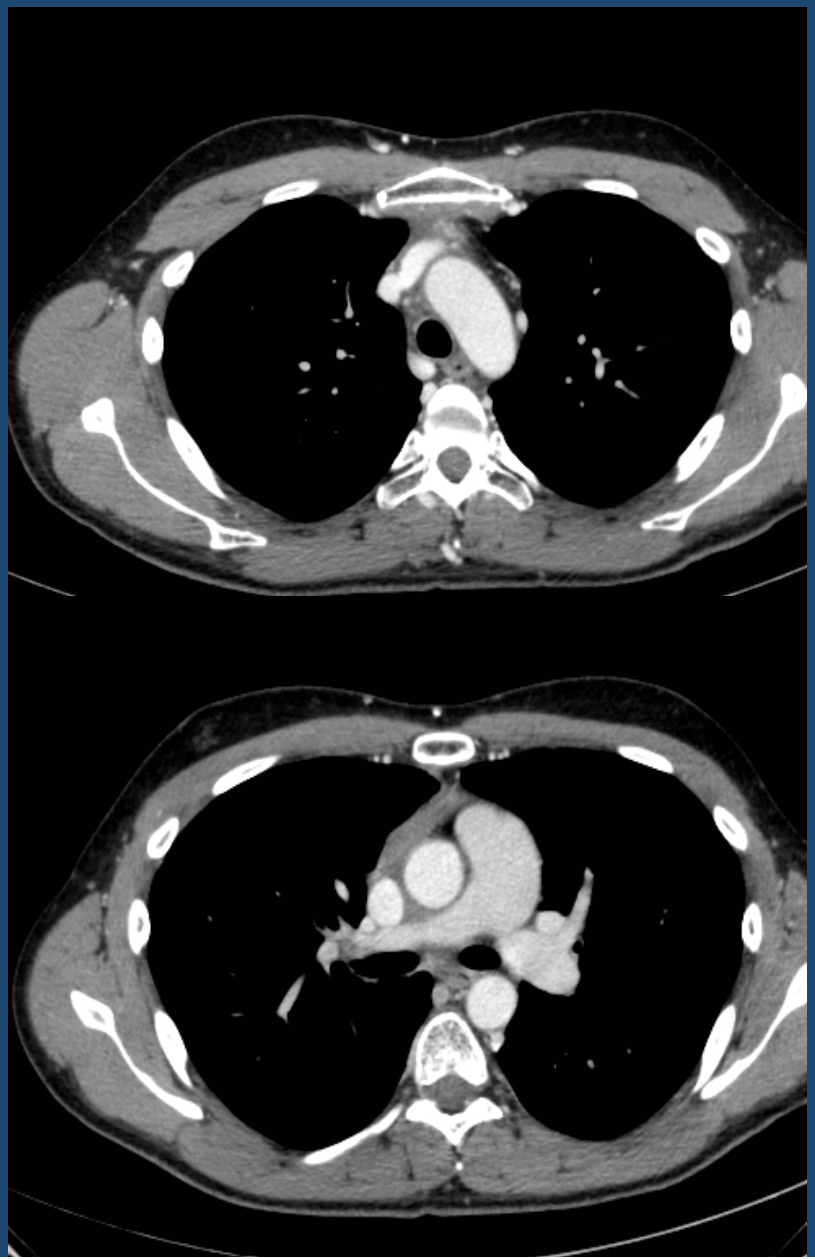

LUNG

- Primary pulmonary L is rare and is encounterd usually in NHL
- Pulmonary involvement is identified more often in HL then in NHL

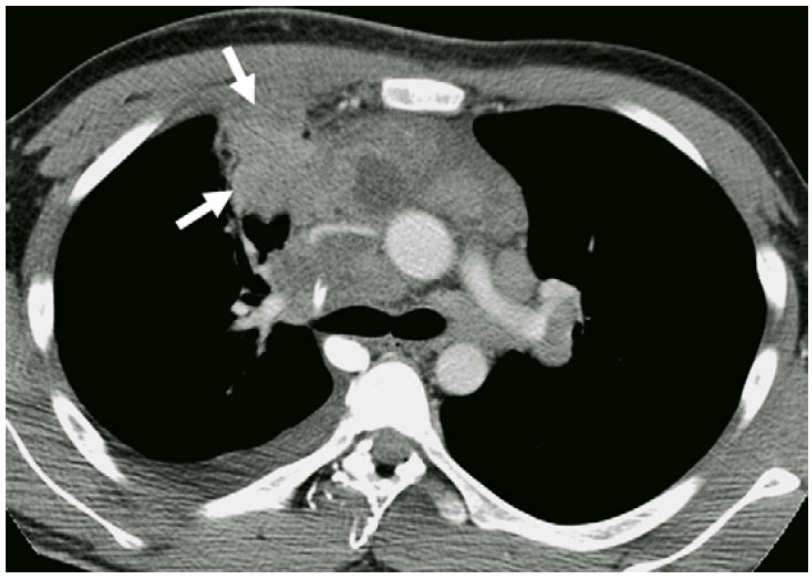

Non-Hodgkin lymphoma (diffuse large B-cell type) showing direct lung involvement from adjacent mediastinal lymphadenopathy in a 17-year-old man. Transverse mediastinal-window CT (5.0-mm section thickness) scan obtained at level of main bronchi shows lymph node enlargement in anterior and middle mediastinal and left hilar areas. Note direct lung involvement from adjacent lymphadenopathy (*arrows*).

- The commonest feature of pulmonary involvement is a direct extension from hilar or mediastinal nodes

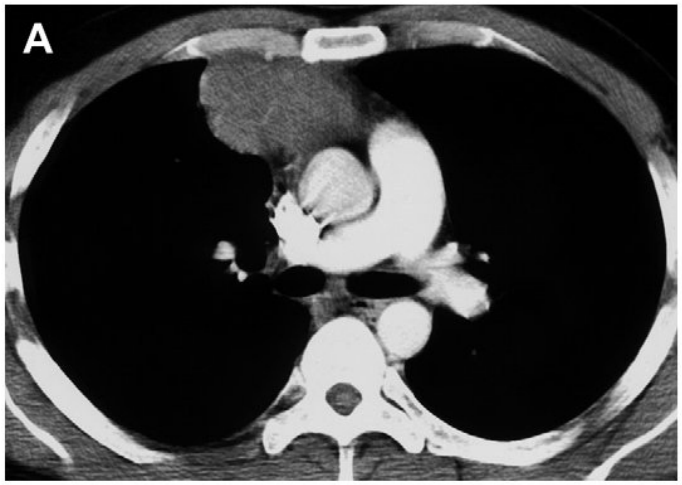

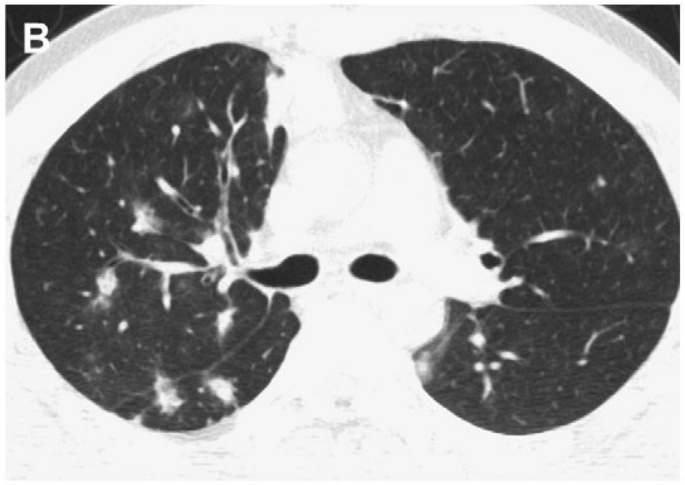

Hodgkin lymphoma (nodular sclerosing type) in a 35-year-old man. (*A*) Transverse mediastinal-window CT (7.0-mm section thickness) scan obtained at level of right upper lobar bronchus shows homogeneous right anterior mediastinal mass. (*B*) Transverse lung-window CT scan shows multiple pulmonary nodules in both lungs with ill-defined margin.

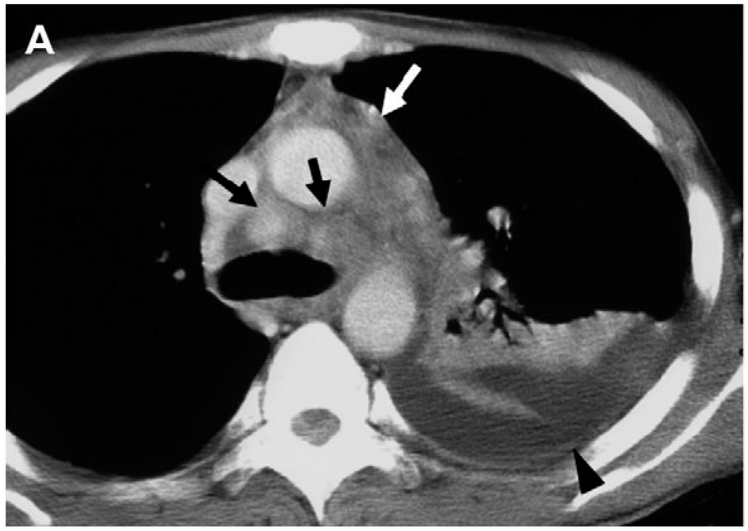

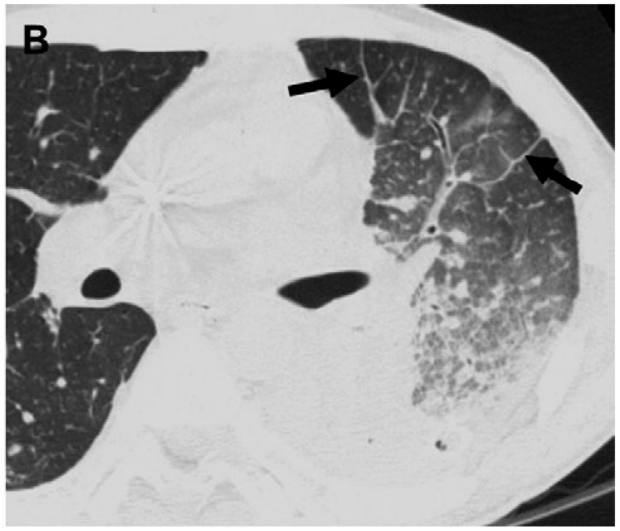

Non-Hodgkin lymphoma (angioimmunoblastic type) in a 33-year-old man. (*A*) Transverse mediastinal-window CT (10-mm section thickness) scan obtained at level of azygos arch shows lymph node enlargement in anterior mediastinal and paratracheal areas (*arrows*). Also note left pleural effusion with pleural thickening (*arrowhead*). (*B*) Transverse lung-window CT scan demonstrates smooth interlobular septal thickening (*arrows*)

69 year-old man with non-Hodgkin's Intravascular large cell lymphoma (ILCL)

Before therapy

After chemotherapy

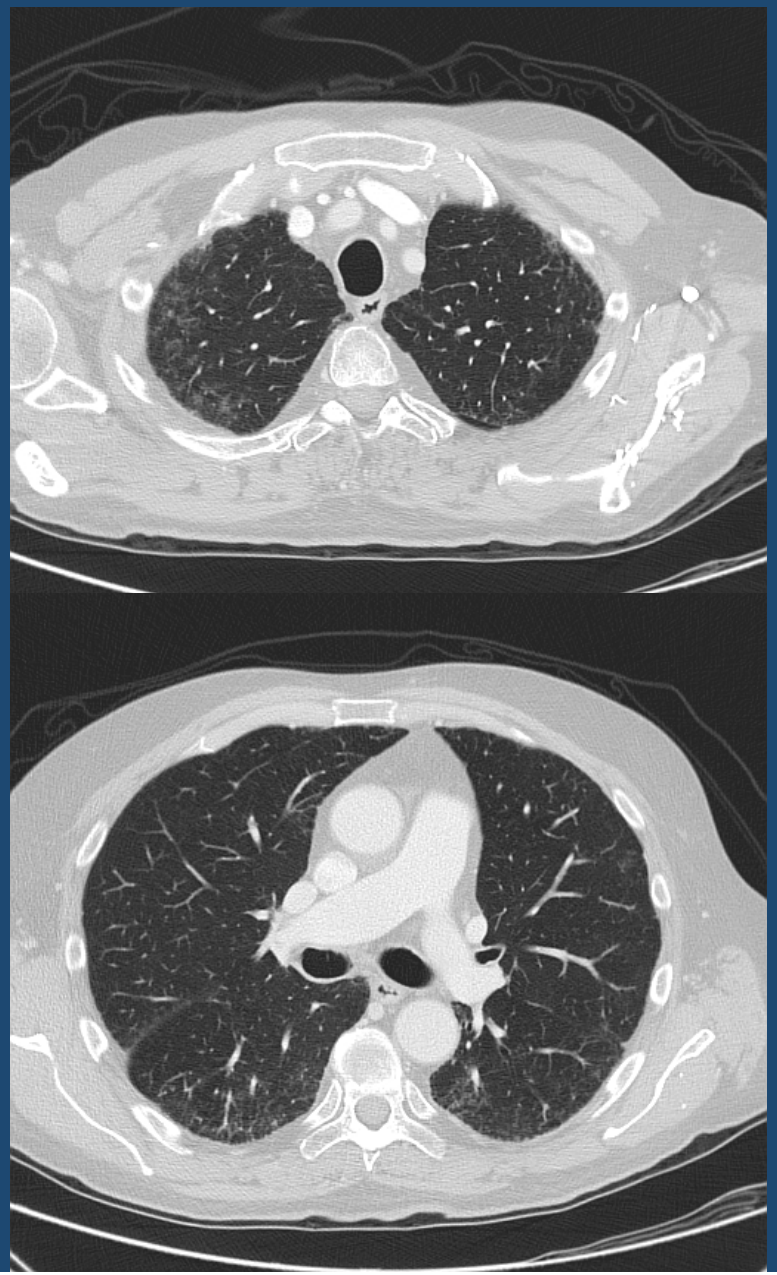

In treated Ps it is often difficult to differentiate between pulmonary involvement and other benign conditions such as infection, radiation pneumonia, or DRUG induced disease.

Imaging of abdominal lymphoma

- Para-aortic LN are the most common findings;
- In general there is displacement of structures by enlarged LN without invasion;
- CT scan, MRI are primarily used to detect LN and the pattern of nodal involvement.

In the abdomen, pelvis, L may present as unifocal, multifocal masses; lymphadenopathy; diffuse infiltration.

LIVER

Rarely L may be a primary lesion.

There are several patterns of hepatic involvement including:

- Hepatomegaly (easily overloked);
- Multifocal hepatic masses (resembling metastases);
- Miliary lesion (d. d. with fungal abscesses);
- Lymphomatous infiltration.

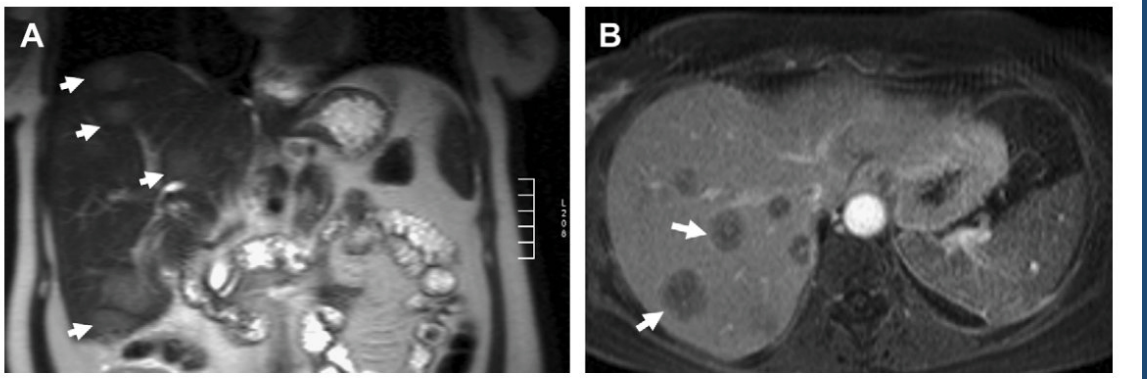

A 50-year-old woman with diffuse large B-cell lymphoma. T2 image (*A*) demonstrates multiple large T2 hyperintense hepatic masses (*arrows*) of varying sizes, which demonstrate hypointense SI on postgadolinium sequence (*arrows*) (*B*).

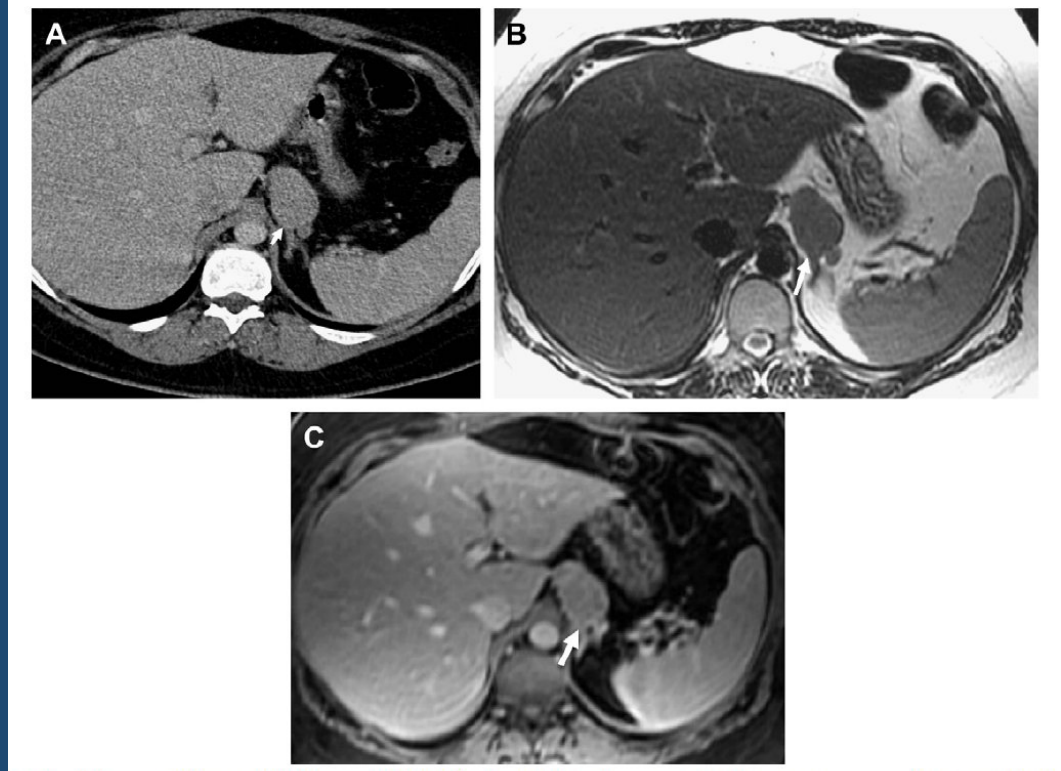

A 40-year-old man with history of NHL. (*A*) CT axial slice demonstrates a homogeneous, well-circumscribed mass (*arrow*) in the left adrenal gland genu. (*B*) The in- and out-of-phase images demonstrated no signal drop out excluding a lipid-containing adenoma. (*C*) The left adrenal mass is slightly T2 hyperintense

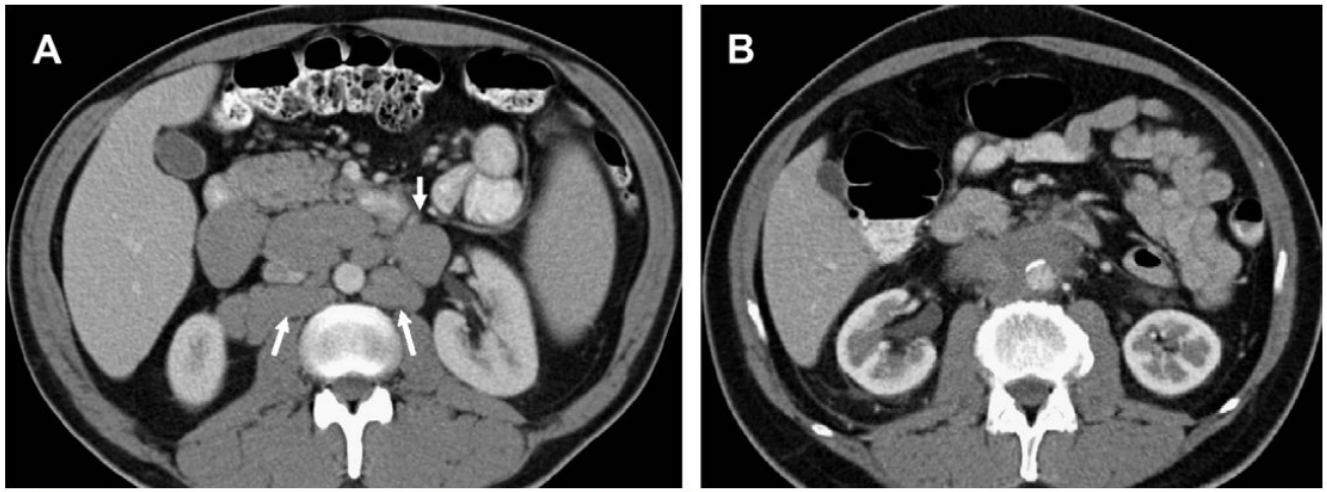

(*A*) CT axial image in a 27-year-old woman with NHL demonstrating extensive retroperitoneal lymphadenopathy (*arrows*), which elevates the aorta from the spine. (*B*) CT axial image in a different patient with biopsy-proved retroperitoneal fibrosis, which is characterized by a mantle of soft tissue encircling the great vessels and ureters in the retroperitoneum. Differentiation from lymphoma, which appears identical in most cases, is made by biopsy.

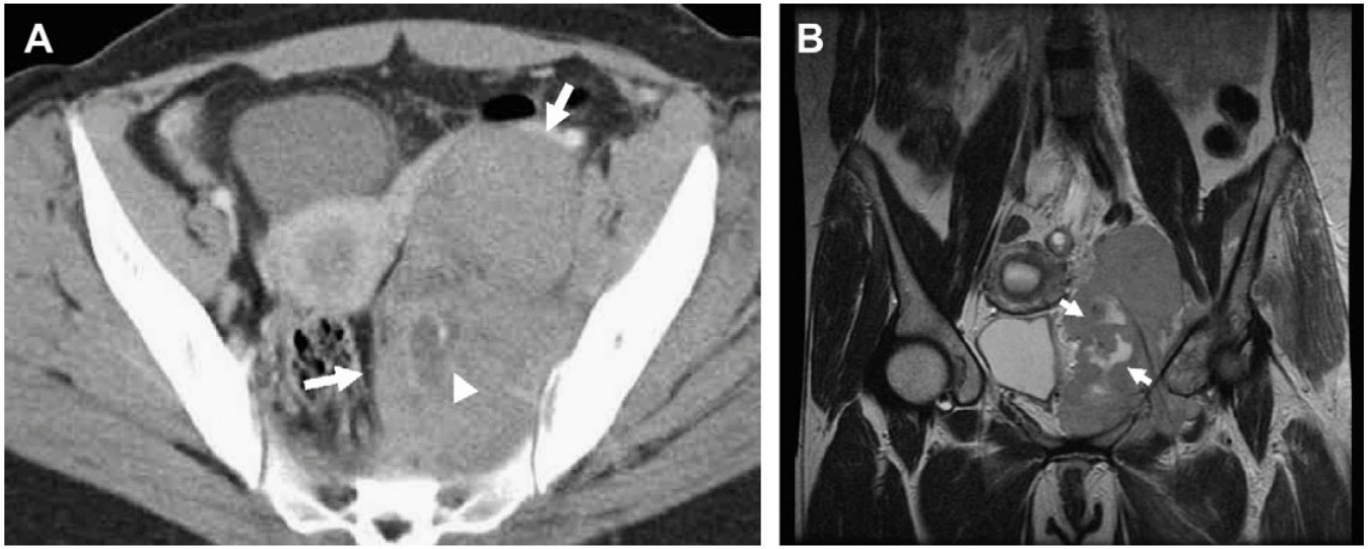

(*A*) CT axial image in a 28-year-old woman with HL with extensive left pelvic wall lymphadenopathy (*arrows*) with areas of hypoattenuation centrally (*arrowhead*). (*B*) MR imaging T2 single shot fast spin echo (SSFSE) axial image demonstrates T2 hyperintense foci suggesting necrosis seen as areas of hypoattenuation on CT (*arrows*).

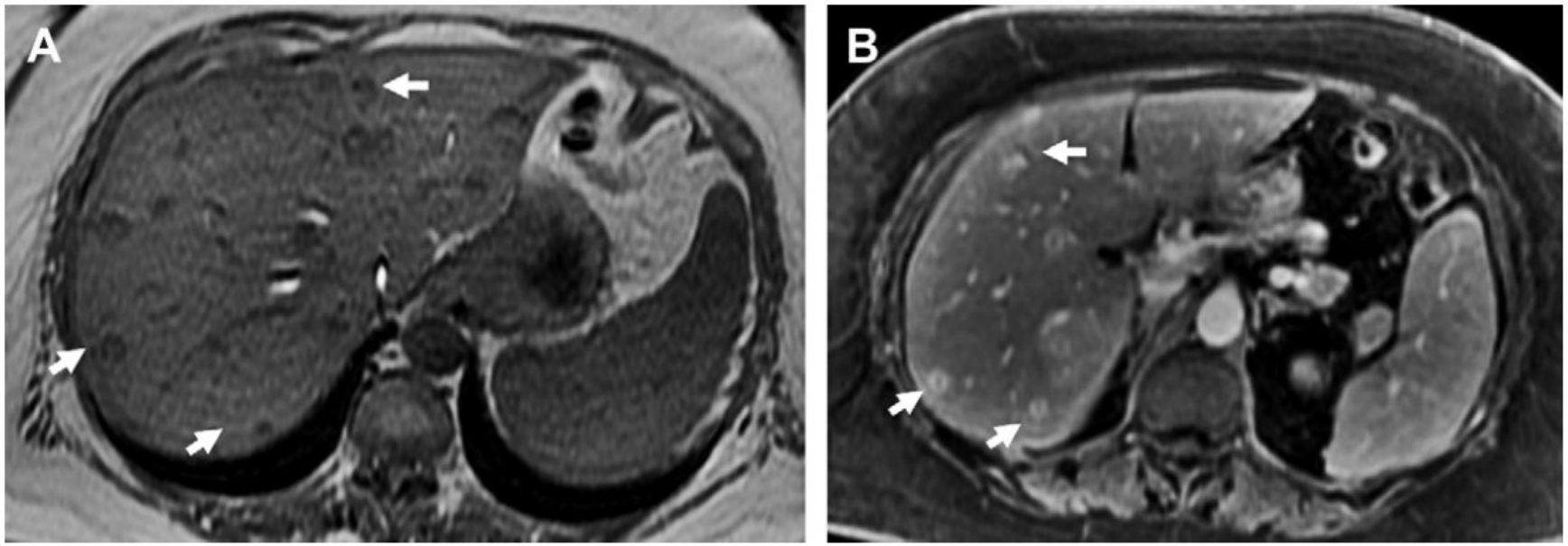

Hepatic fungal abscesses in a patient with NHL status postchemotherapy presenting with fever and right upper quadrant pain. (*A*) T1 gradient echo sequence demonstrating multiple T1 hypointense subcentimeter hepatic lesions (*arrows*) in this patient with NHL on chemotherapy presenting with fever. (*B*) Postgadolinium image shows these lesions to be rim enhancing (*arrows*).

Imaging appearance of L of the spleen:

- Splenomegaly;
- Solitary mass;
- Multifocal nodules;
- Diffuse infiltration
- NHL is the most common tumor;

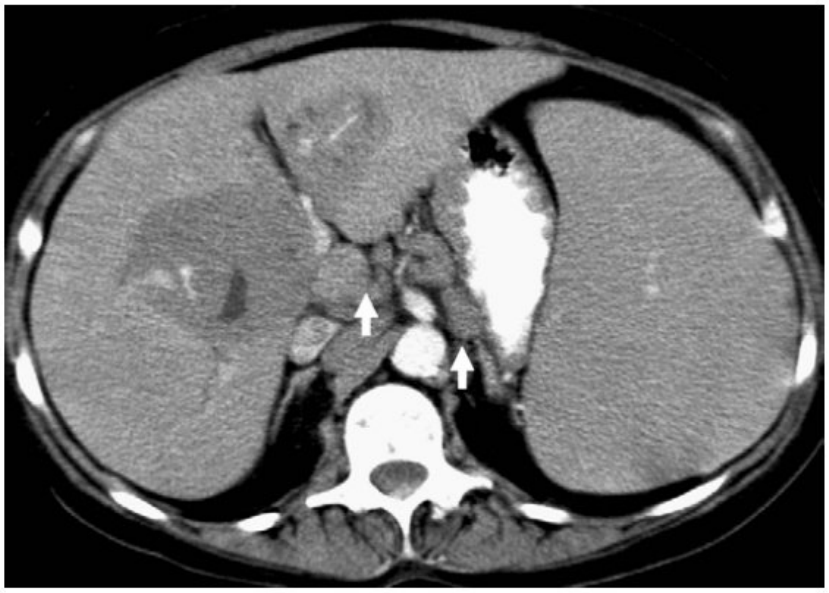

NHL in a 40-year-old man presenting as an infiltrative mass emanating from the porta hepatis and splenomegaly. Celiac axis lymphadenopathy (*arrows*) is also evident.

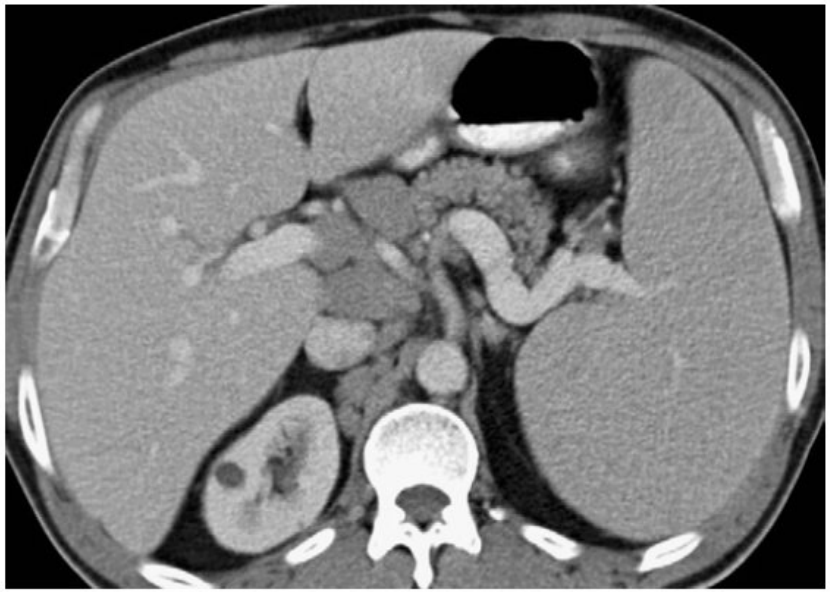

Fig. 13. CT axial image in a 27-year-old woman with NHL with extensive porta hepatis lymphadenopathy and splenomegaly.

Axial CT image in a 50-year-old man with HL presenting as multiple hypodense masses in the spleen. Multiple large porta hepatis and mesenteric nodes are also evident (*arrows*).

Pancreas - Gastric - Small bowel - colon, mesentery

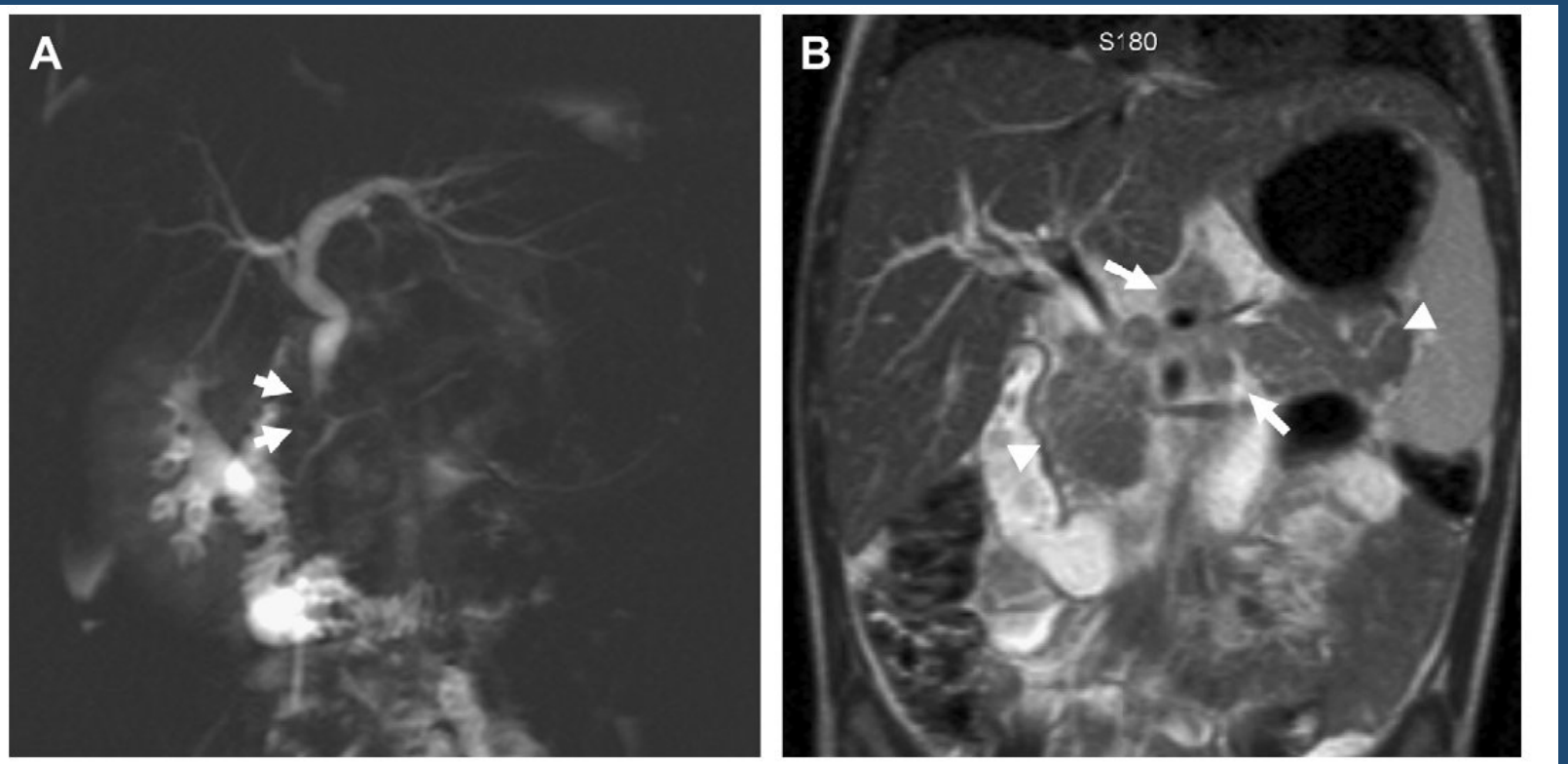

Anaplastic large cell lymphoma. Magnetic resonance cholangiopancreatography (*A*) and coronal T2 fast spin echo (*B*) sequences. MRCP image (*A*) shows a narrowing in the distal common bile duct related to extrinsic compression and is slightly enlarged with minimal intrahepatic biliary dilatation; the pancreatic duct is normal. T2 coronal sequence demonstrates pancreatic enlargement (*arrowheads*) and peripancreatic lymphadenopathy (*arrows*) without associated pancreatic duct dilation.

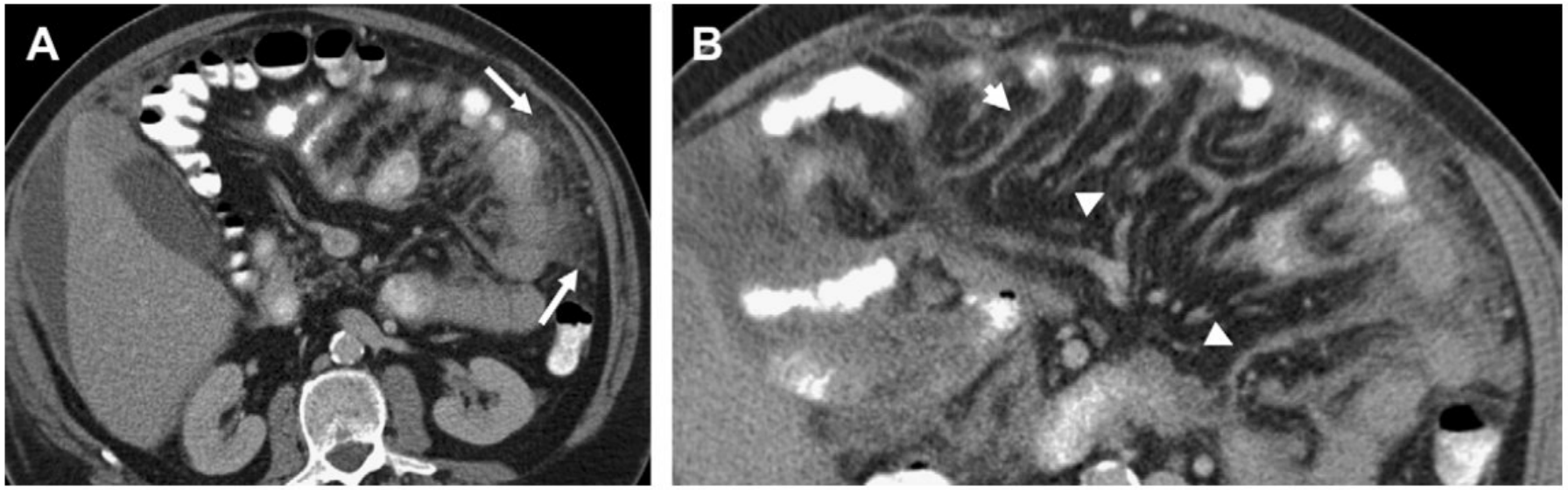

(*A*, *B*) A 40-year-old man with NHL presenting as mesenteric lymphoma, which typically spreads as sheets along the peritoneal surface causing a rigid pleating of thickened mesenteric leaves (*arrowheads*). Arrows mark the omental disease.

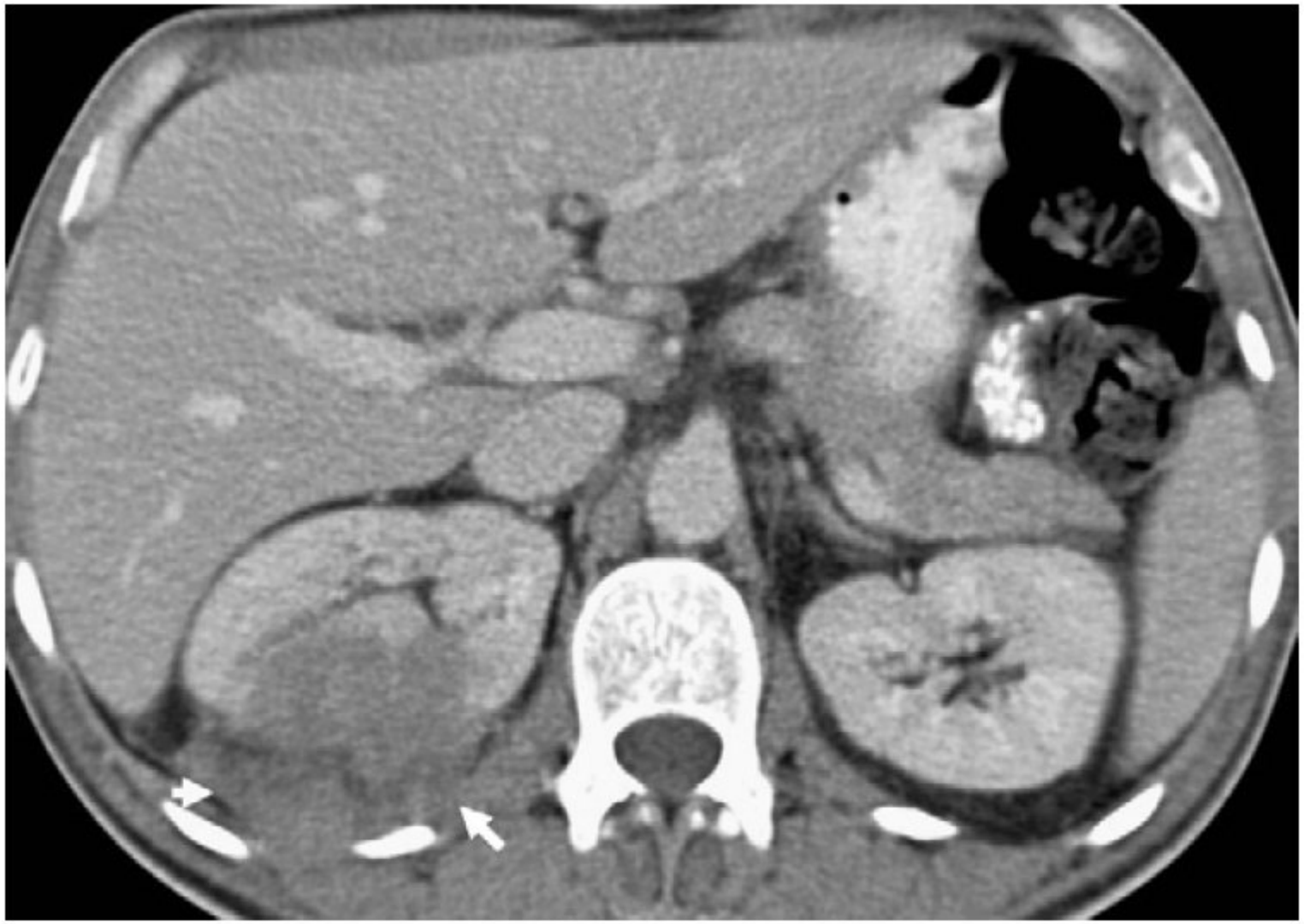

CT axial image in a 54-year-old man with B-cell lymphoma presenting as a focal right kidney (*arrows*) with extension into the retroperitoneum.

47 year-old man with diffuse large B-cell lymphoma (DLBCL) localized to ileum and colon (stage IVa)

Before therapy

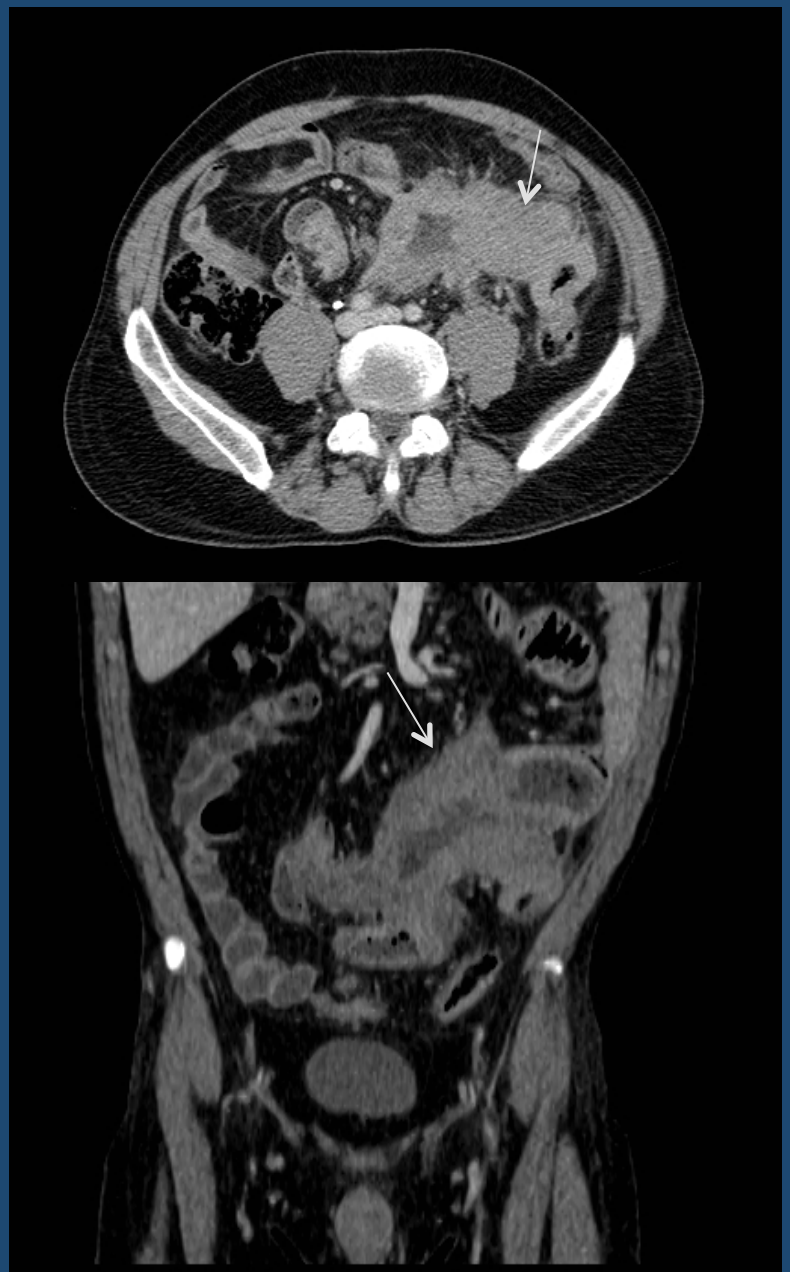

After chemotherapy

81 year old man with diffuse large B-cell lymphoma (DLBCL) localized to lymph node, gastric and ileal.

Before therapy

After chemotherapy

A 63-year-old woman with lymphoma of the bladder (concurrent low-grade mucosa-associated lymphoid tissue lymphoma and aggressive diffuse large cell lymphoma) presenting as focal thickening of the anterior wall of the urinary bladder (*arrows*).

“Traditional” MR imaging

- The accuracy in detecting LN and organ involvement is similar to that of CT;
- Lymphoma masses: low to iso-signal intensity on T1-weighted images, and moderately high signal on T2;
- Tumor masses are hyperintensive on T2-WI, and chronic fibrosis or scar are often hypointense.

The mean Gd enhancement of residual masses after treatment is often substantially weaker than that observed before treatment in Ps in complete remission

The sensitivity of these findings is low because of necrosis, immature fibrotic tissue, edema, inflammation that can simulate the high T2 signal intensity of a viable tumor.

Diffusion-weighted (DW) MRI non invasively depicts the random microscopic motion of water molecules in the body, which depends on cellularity and cell membrane integrity.

Because of their high cellularity and high nucleus-to-cytoplasm ratio, lymphomas have a lower apparent diffusion coefficient (ADC) value than do other tumors.

The restricted diffusion of water molecules is proportional to the degree of cellularity of the tissue and the integrity of the cell membranes.

Decreased cell proliferation and cell density in treated tumors could induce a change in signal intensity on DW imaging.

DWI → two additional large gradients are placed on each side of a 180 degree pulse;

B-value → is a factor that reflects the strength and timing of the gradients used to generate DWI;

ADC MAPS → acquisition of multiple imaging with different b value. Is a measure of magnitude of diffusion of water molecoles within tissue.

Lesion type	*b* = 50	*b* = 400	*b* = 800	ADC
Benign lesion	○	●	●	○
Lymphoma	○	○	○	●
Lesion with long T2 relaxation time	○	○	○	○

Chart compares lesion signal intensity on DW images and ADC maps. Benign lesions show a decrease in signal intensity (progressively shaded circles) as the *b* value increases and are hyperintense (white circles) on ADC maps, whereas lymphomas are hyperintense at all *b* values and hypointense relative to muscle on ADC maps. Lesions with long T2 relaxation times may be hyperintense at all *b* values and hyperintense on ADC maps because of T2 shine-through effect.

- Radiologists should interpret DWI in conjunction with ADC MAPS

Tauli B et al. *Radiology* 2010; 254(1):47-66.

Decrease in ADC value reflects an increase in total cellular size or number, as is seen with tumor progression.

In contrast increases in ADC values reflect a successful treatment of lymphoma.

An increase in ADC values is observed, after chemoth, much earlier than morphologic change.

Rapid technical developments, such as echo-planar sequences, parallel imaging, multichannel phased array surface coils, respiratory gating, moving examination tables …

Whole body diffusion-weighted (DW) MR that reflects cell density is now feasible in routine clinical practice.

Scout DW images obtained with a platform setup at 3-T whole-body DW imaging. Seven to eight stations are used to cover the entire body from the neck to the upper thighs. Each station is 11 cm long and comprises 22 5-mm-thick contiguous sections. The neck station is oblique so that it is perpendicular to the cervical vessels.

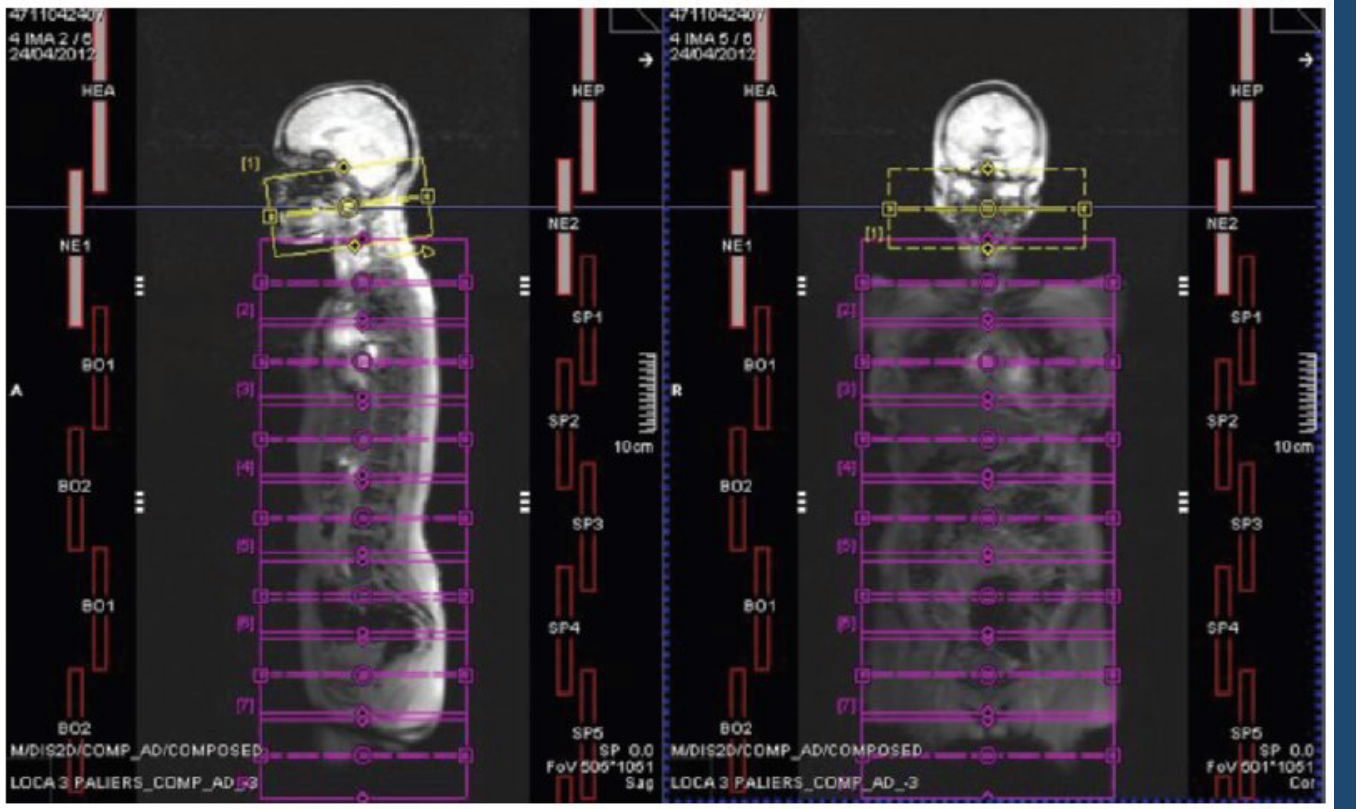

Toledano S – Massia M et al. Radiographics. 2015; 35:747-764.

Recent studies showed that WBDW imaging was not only comparable to PET/CT in Ps with FDG-avid lymphoma but also was superior in Ps with lymphoma subtypes with variable FDG avidity.

MAYEROEFER ME et al. Clin Cancer Res 2014; 20(11): 2984-2993.

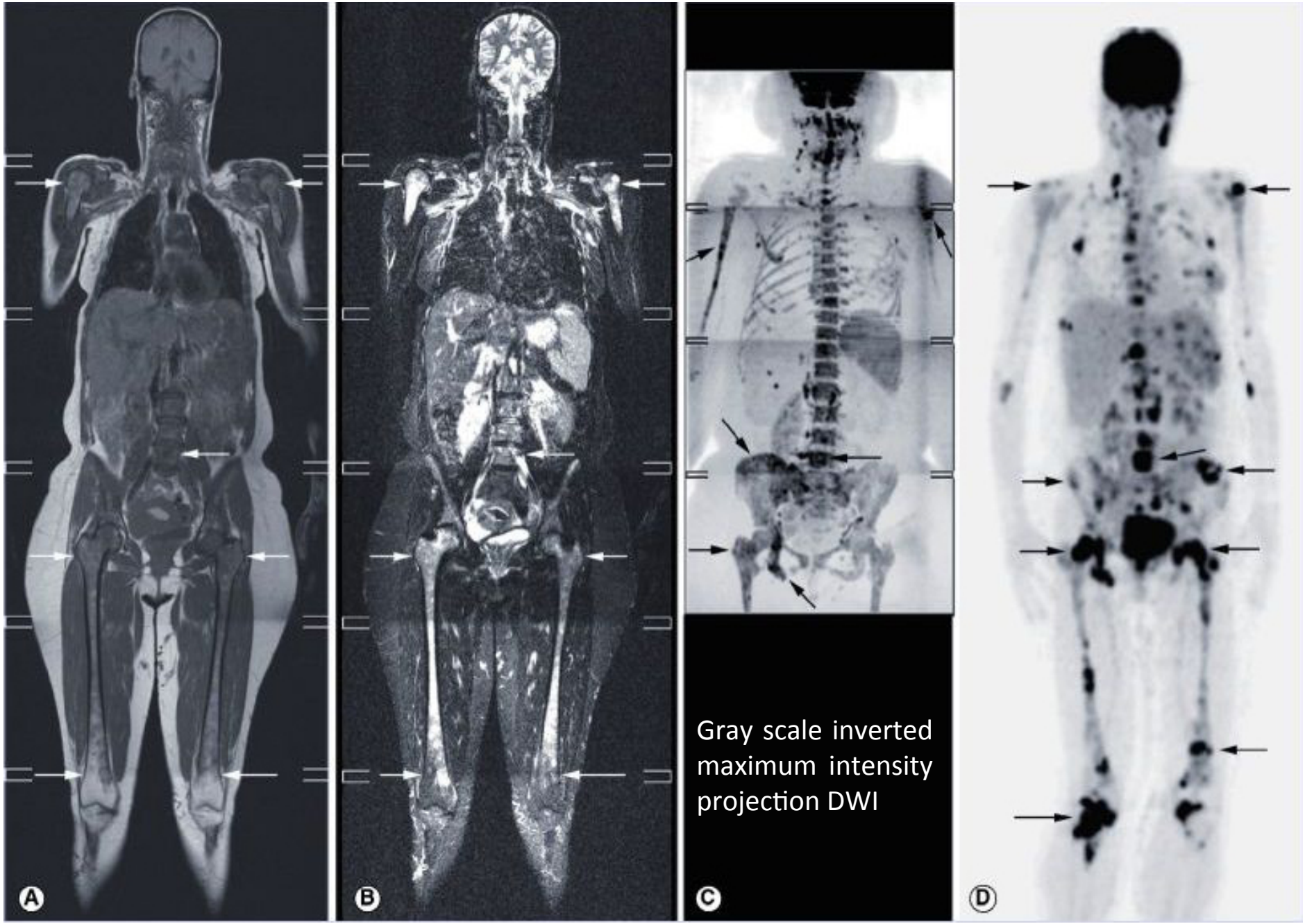

Vermoolen MA, Kersten MJ, Fijnheer R et al. Magnetic resonance imaging of malignant lymphoma. Expert Rev Hematol. 2011;4(2):161-171.

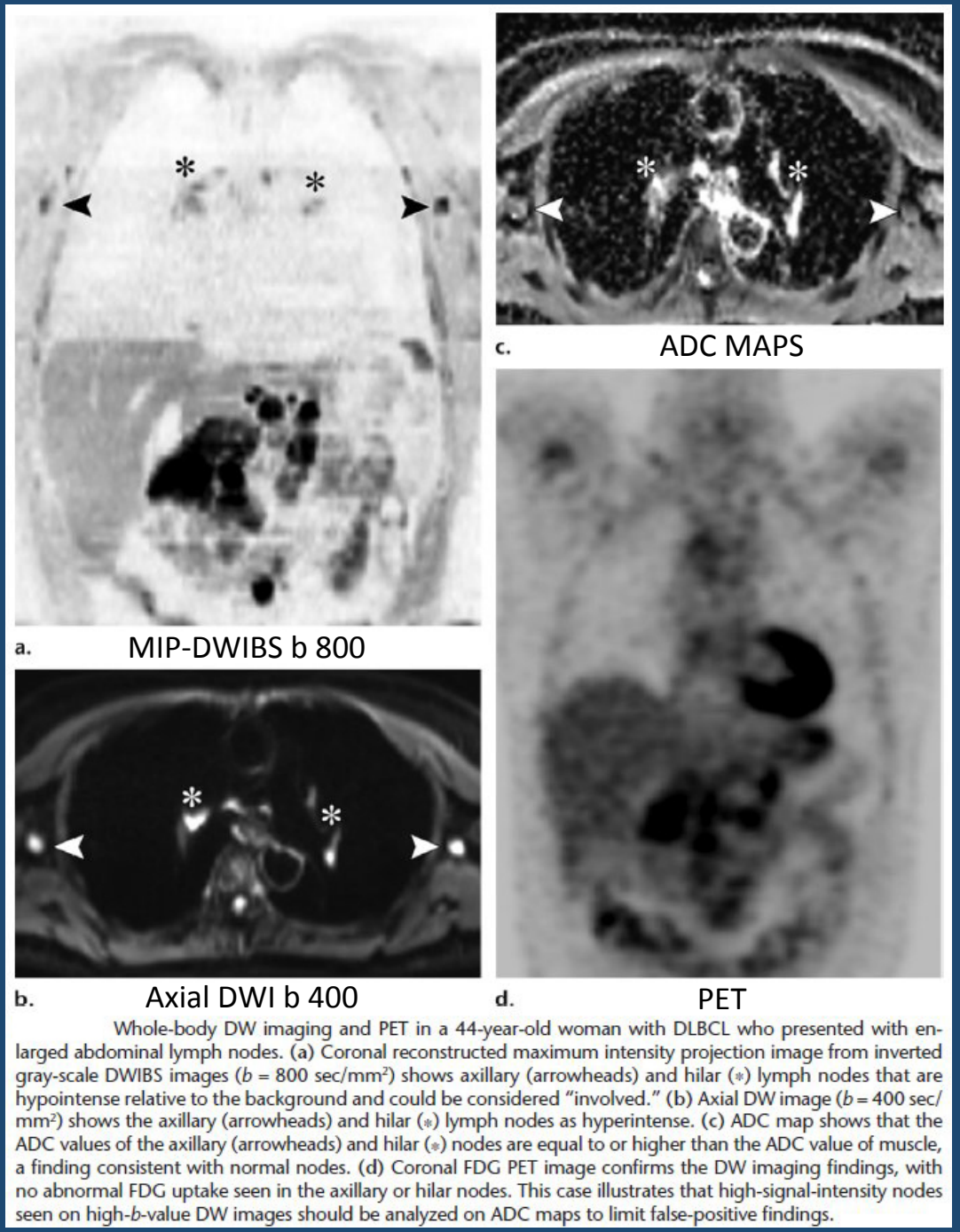

Whole-body DW imaging and PET in a 44-year-old woman with DLBCL who presented with enlarged abdominal lymph nodes. (a) Coronal reconstructed maximum intensity projection image from inverted gray-scale DWIBS images (b = 800 sec/mm^2) shows axillary (arrowheads) and hilar (*) lymph nodes that are hypointense relative to the background and could be considered "involved." (b) Axial DW image (b = 400 sec/mm^2) shows the axillary (arrowheads) and hilar (*) lymph nodes as hyperintense. (c) ADC map shows that the ADC values of the axillary (arrowheads) and hilar (*) nodes are equal to or higher than the ADC value of muscle, a finding consistent with normal nodes. (d) Coronal FDG PET image confirms the DW imaging findings, with no abnormal FDG uptake seen in the axillary or hilar nodes. This case illustrates that high-signal-intensity nodes seen on high-b-value DW images should be analyzed on ADC maps to limit false-positive findings.

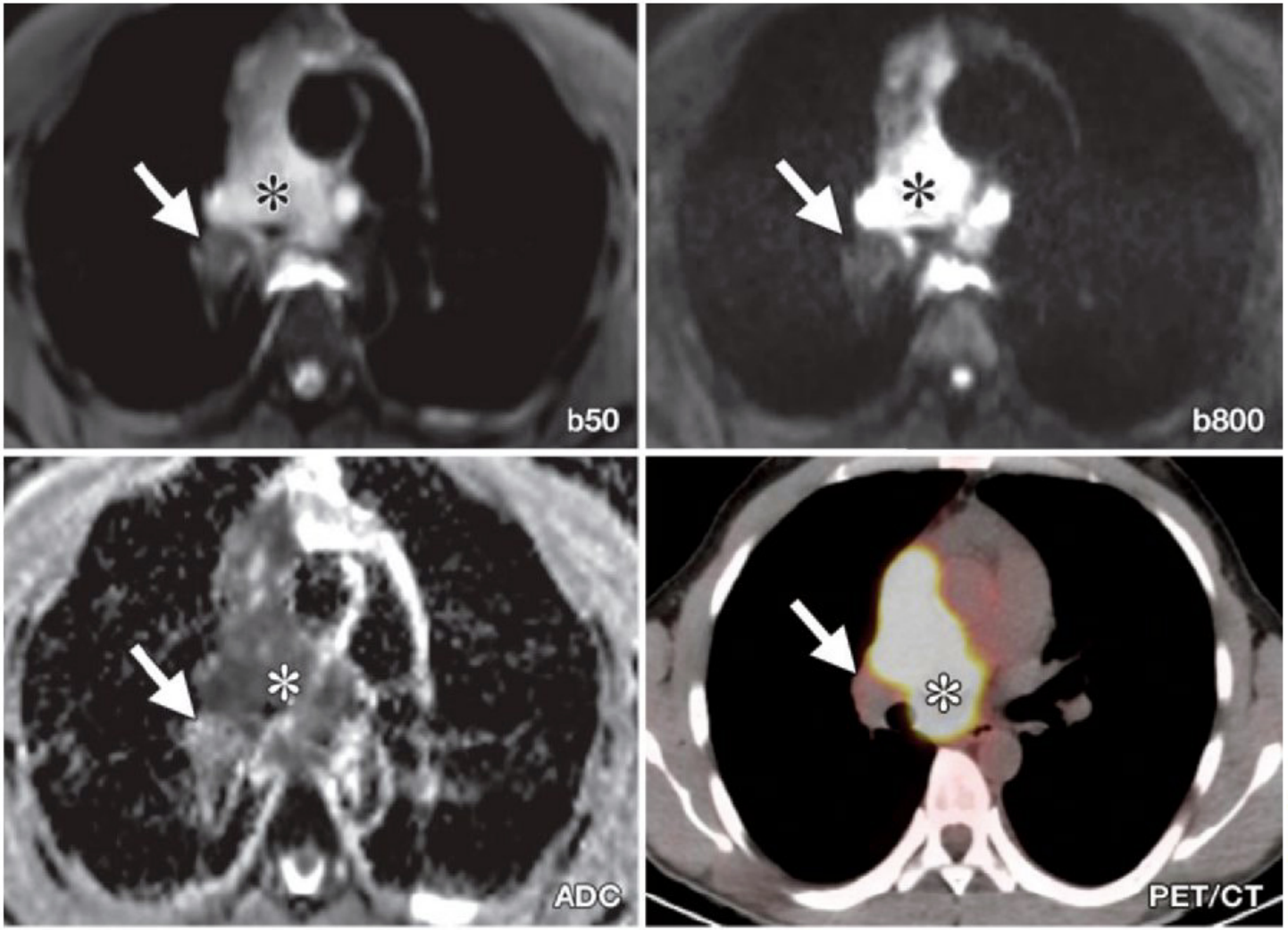

a.

Lymph node characterization in a 34-year-old man with DLBCL. **(a)** Axial baseline images show enlarged mediastinal paratracheal lymph nodes (*) that are hyperintense on 1.5-T DW images (b = 50 sec/mm^2, top left; b = 800 sec/mm^2, top right) and hypointense on an ADC map (bottom left), with intense FDG uptake seen on a PET/CT image (bottom right). The right hilar lymph node (arrows) is isointense relative to muscle on the DW images and ADC map, with no abnormal FDG uptake seen on the PET/CT image.

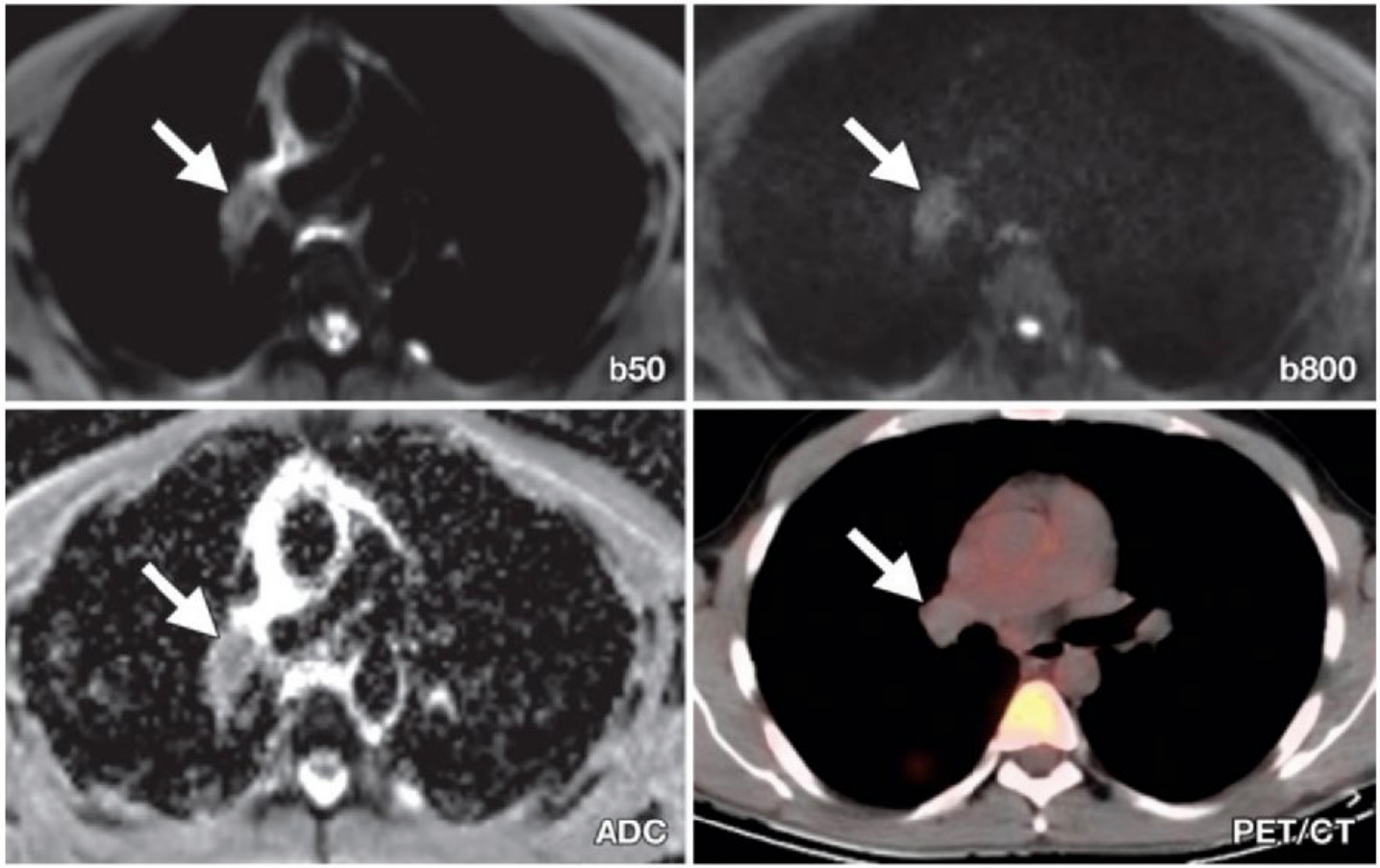

b.

(b) Axial images obtained after two cycles of chemotherapy show that the size of the right hilar node (arrows) remains unchanged on a DW image (b = 50 sec/mm^2; top left), with decreased signal intensity seen on a high-b-value DW image (b = 800 sec/mm^2; top right), elevated signal intensity on an ADC map (bottom left), and reduced FDG uptake on a PET/CT image (bottom right). The findings are consistent with a benign node.

Treatment response in a 28-year-old woman with stage IV Hodgkin lymphoma. (**a**, **b**) Axial 3-T DW image (b = 50 sec/mm^2) (**a**) and ADC map (**b**) obtained at the end of treatment show an anterior mediastinal mass (arrow) not present before treatment that is hyperintense relative to muscle on the ADC map, with no restricted diffusion. (**c**) Axial DW images show a decrease in signal intensity in the mass (arrows) between in-phase (left) and out-of-phase (right) T1-weighted images, a finding that confirms the fatty content of the mass. (**d**) Axial PET/CT image shows abnormal FDG uptake in the mass. The mass was considered to represent thymic rebound, and no change was made in the treatment strategy.

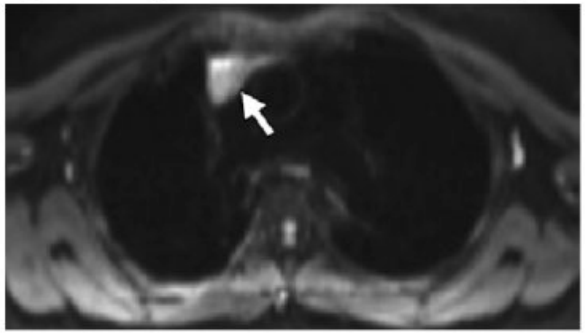

a.

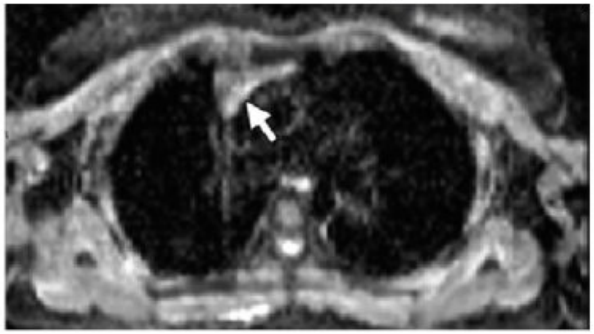

b.

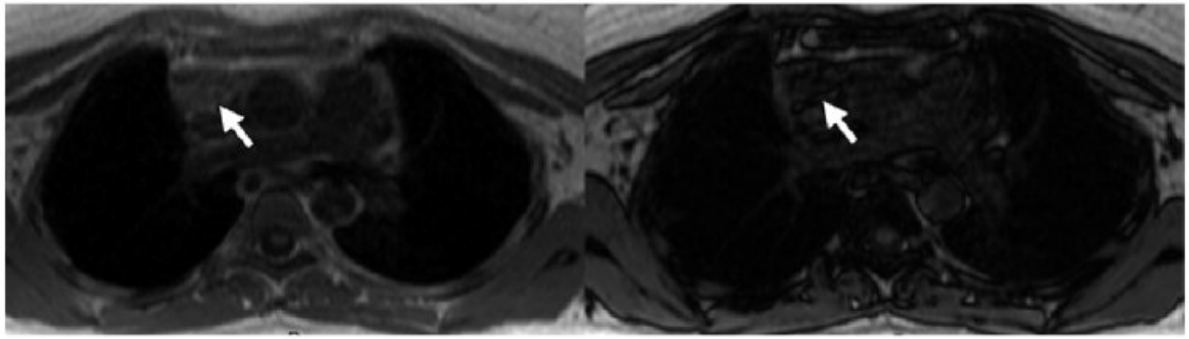

c.

d.

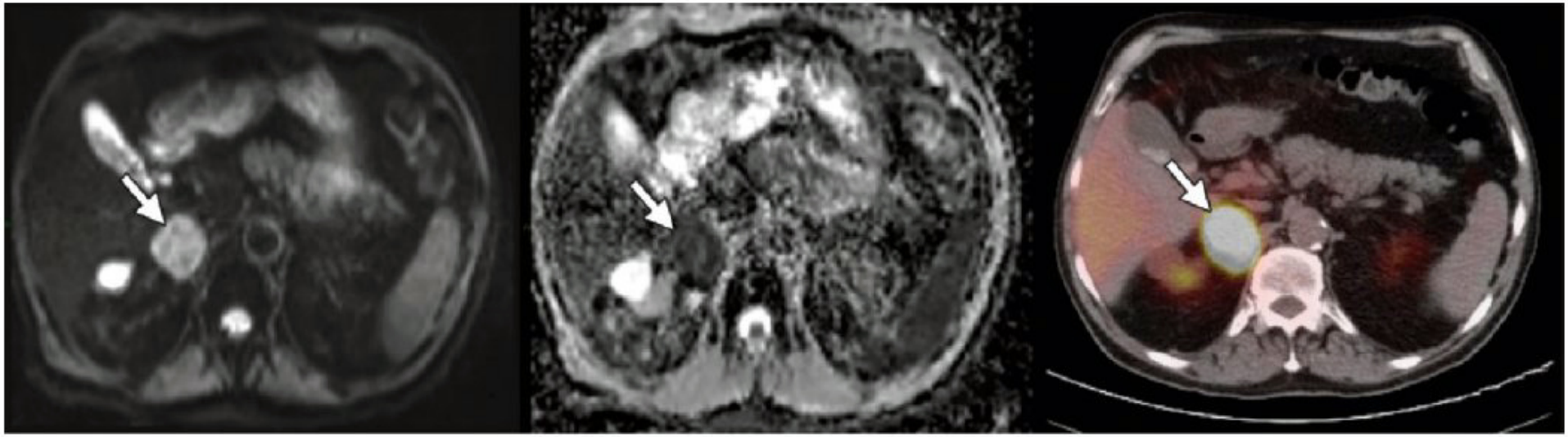

a.

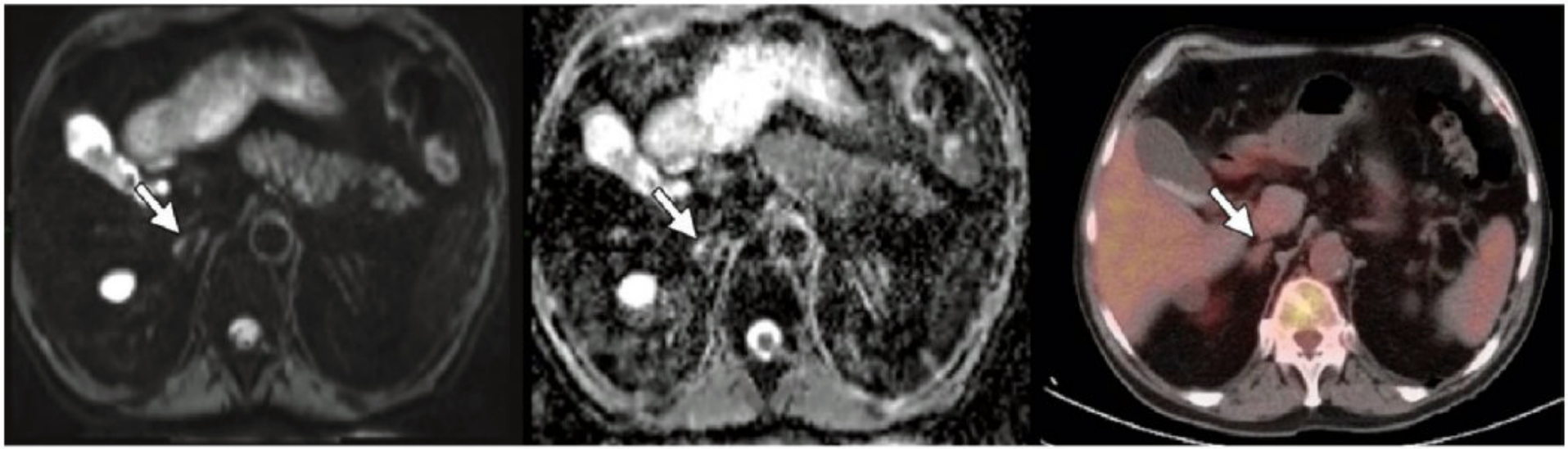

b.

Treatment response in a 77-year-old man with DLBCL. (**a**) Axial pretreatment 3-T DW image (b = 50 sec/mm^2) (left) and ADC map (middle) show an enlarged right adrenal gland (arrows) that is hyperintense on the DW image and hypointense on the ADC map, with intense FDG uptake seen on a PET/CT image (right). (**b**) Axial posttreatment 3-T DW image (b = 50 sec/mm^2) (left) and ADC map (middle) show that the right adrenal gland (arrows) has returned to normal size with no restricted diffusion. No abnormal FDG uptake is seen on a PET/CT image (right).

MR artifacts and Pitfalls

Patient-dependent factor

- Foreign body artifact
- False positive lesion

Technique dependent factors

- T2 shine-through effect
- Motion related artifact
- Iron and calcium containing lesion

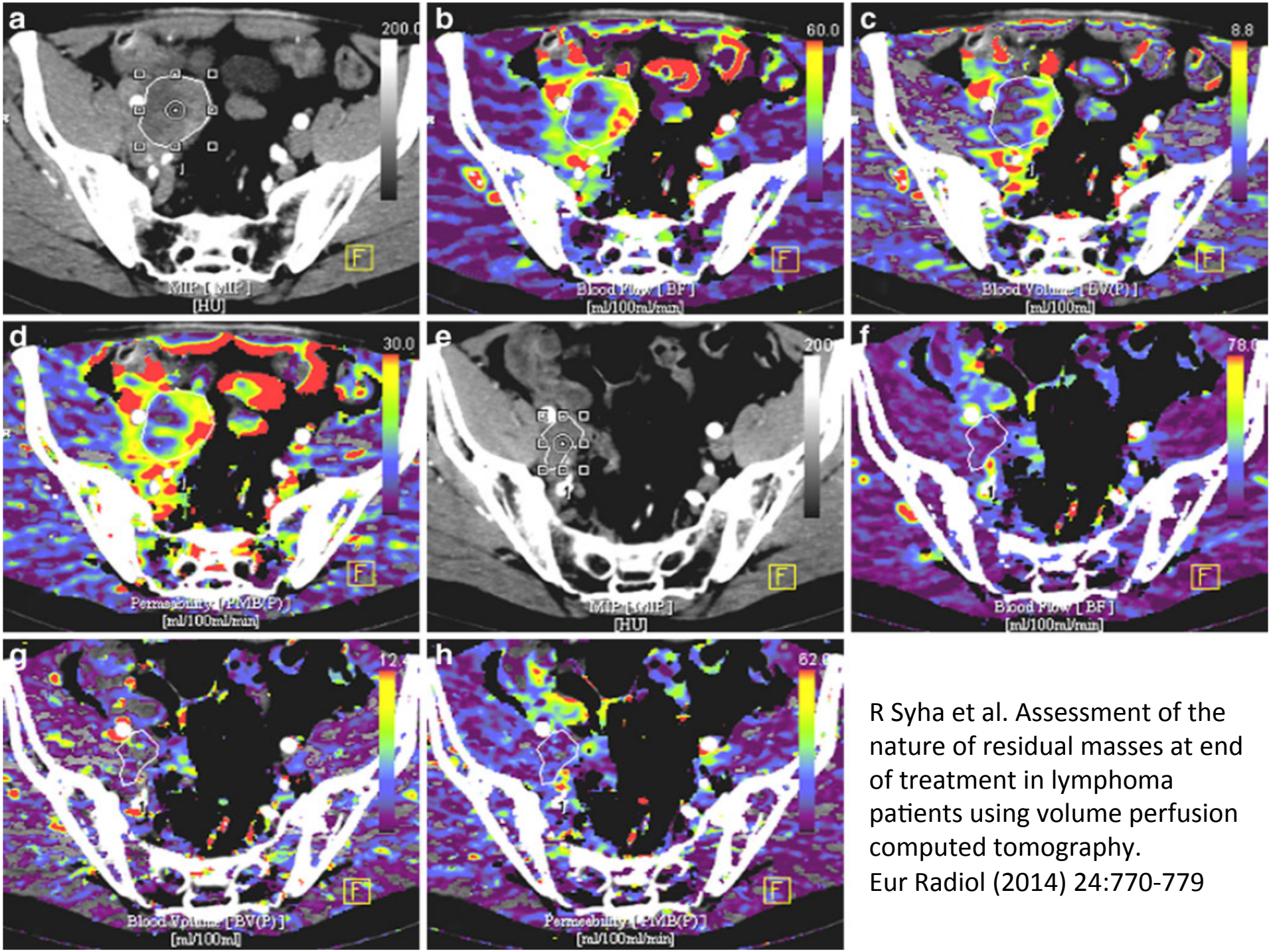

R Syha et al. Assessment of the nature of residual masses at end of treatment in lymphoma patients using volume perfusion computed tomography.
Eur Radiol (2014) 24:770-779

Conclusion

MRI + DWI is emerging as powerful clinical tool in the care of patients with cancer and can provide important information related to tumor cellularity and integrity of the cellular membrane.

In Ps with lymphoma, whole-body DWI can be clinically useful for disease detection, lesion characterization and assessment of tretment response. However careful optimization of this technique is required to ensure high-quality images.

Furthermore, hybrid PET/MR imaging could provide complementary functional and anatomic information and be a valuable aid in the treatment of patients with lymphoma.

Computed Tomography

WB - DWI / MRI

- Increase radiologist acceptance
- Clinically acceptable scan time possible
- STIR type fat-suppression preferred
- Avoid false positive reading by:
- Correlation with anatomical sequences
- Knowledge of anatomy and phisiology
- Supportive problem solver → PET/MRI?

PET / CT

COMPETITIVE OR COMPLEMENTARY ?

References

- YA Bae, KS Lee; Cross-sectional evaluation of thoracic lymphoma. *Radiol Clin N Am* 2008; 46(2):253-64.
- M Anis, A Irshad; Imaging of abdominal lymphoma. *Radiol Clin N Am* 2008; 46:265-285.
- S Toledano-Massiach et al.; Wole-body diffusion-weighted imaging in hodgkin lymphoma and diffuse large b-cell lymphoma. *Radiographics* 2015; 35:747-764.
- HM Van Uffold et al.; Newli diagnosed lymphoma: initial results with whole-body T1 weighted, STIR, and DW MRI compared with 18F-FDG PET/TAC. *AJR* 2011; 196(3):662-669.
- C Lin et al.; Whole.body diffusion magnetic resonance imaging in the assessment of lymphoma. *Cancer Imaging* 2012; 12(2):403-408.
- ME Mayerhoefer et al.; Evaluation of diffusion weighted MRI for pretherapeutic assessment and staging of lymphoma: resuslts of a prospective study in 140 patients. *Clin Cancer Res* 2014; 20(11):2984-2993.

- C Lin et al.; Whole-body diffusion-weighted magnetic resonance imaging with apparent diffusion coefficient mapping for staging patients with diffuse large b-cell lymphoma. *Eur Radiol* 2010; 20(8):2027-2038.
- AR Padhani et al.; Diffusion MR imaging for monitoring of treatment response. *Magn Reson Imaging Clin Nam* 2011; 19(1):181-209.
- DA Hamstra et al.; Diffusion magnetic resonance imaging: a biomarker for treatment response in oncology. J Clin Oncol 2007; 25(26): 4104-4109.
- M Horger et al.; Very early indicators of response to systemic therapy in lymphoma patients based on alterations in water diffusivity: a preliminary experience in 20 patients undergoing whole-body diffusion-weighted imaging. *Eur J Radiol* 2014; 83(9):1655-1664.
- MA Vermoolen et al.; MRI of malignant lymphoma. Expert review of hematology 2011; 4(2): 161-171.
- RB Lewis et al.; From the radiological pathology archives. Gastrointestinal lymphoma: radiologicand phathologic findings. Radiographics 2014; 34:1934-1953.
- J Rademaker et al.; Hodgkin's and non Hodgkins Lymphpmas. *Radiol clin N Am* 2007; 45:69-83.